Research on the Optimal Design of Heliostat Field Based on Simulated Annealing Algorithm

Shanwei Nan *

School of Biological Engineering and Food, Hubei University of Technology, Wuhan, China

* Corresponding Author Email: 1375647241@qq.com

Abstract. This paper focuses on the optimized design of the heliostat field in depth. First, the spatial relationship between the sun and the heliostat mirror field is determined by calculating the sun's declination, altitude, and azimuth angles, as well as the normal direct radiation irradiance (DNI). Second, the shadow obscuration area and the annual average optical efficiency of each mirror were determined by vector differentiation and mechanistic analysis, combined with Monte Carlo methods. Finally, optimization calculations were performed using a simulated annealing algorithm to derive the optimal values of each decision variable and the corresponding annual average output thermal power.

Keywords: Fixed-heaven mirror field, optical efficiency, simulated annealing algorithm, thermal power.

1. Introduction

In the face of global climate change and environmental pressures, tower solar photovoltaic (PV) power plants are gradually gaining attention, especially in terms of optimizing performance to reduce energy costs and mitigate climate change [1]. This study focuses on a specific circular heliostat mirror field with geographic coordinates of 98.5°E, 39.4°N, an elevation of 3000 m above sea level, and a radius of 350m [2]. The objectives of the study are to calculate the annual average optical efficiency, the annual average output thermal power, and the annual average output thermal power per unit mirror area. In addition, the study involves the design of a heliostat mirror field capable of achieving a rated annual average output thermal power of 60 MW, as well as the determination of the associated optimization parameters.

2. Planning models based on light efficiency and geographic coordinates

In solving for the annual average optical efficiency, this study first decomposes and calculates the optical efficiency of each heliostat based on a specific optical efficiency formula, considering the potential effects of various factors on optical efficiency. By combining the geometry of the incident and reflected light from the mirrors and the given efficiency formulae, the relevant parameters and angular data are solved accurately. Further, optical efficiencies were also calculated in this study at different points in time during the day, with special attention paid to variations in the light-gathering area. Since there is no heliostat within 100 meters of the absorb tower, the absorb tower has no effect on the light harvesting area. In this regard, the study modeled the light harvesting area especially for the shading between adjacent heliostats and the pitch angle of the plane mirror.

2.1. Calculation of solar position parameters

2.1.1 Solar Position Model

Calculate the solar altitude angle ST and the solar azimuth angle α_s for each time point γ_s , using the provided formulas, the geometric relationships of which are shown in Fig. 1.

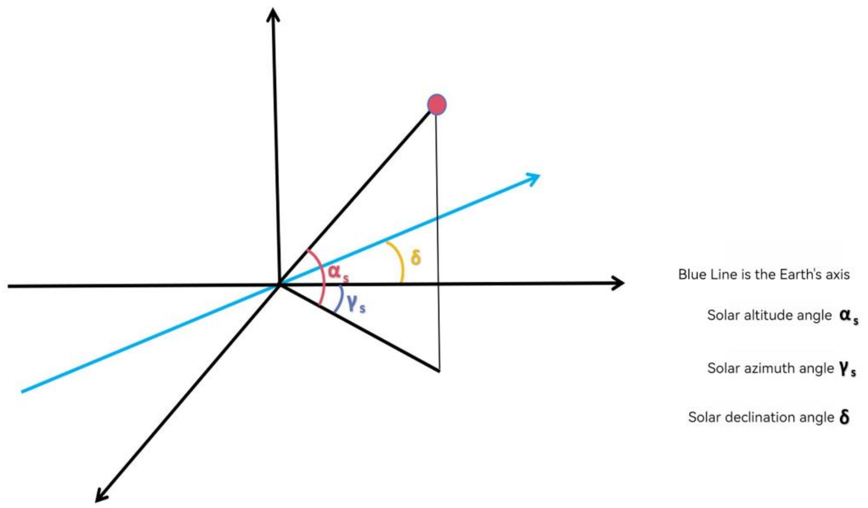

Fig. 1 Angle-position relationship

Known latitude = 39.4°
Solar altitude angle:

$$\sin\alpha_s = \cos\delta_m \cos\varphi \cos\omega_n + \sin\delta_m \sin\varphi \quad m = 1,2\ldots12; \ n = 1,2\ldots5 \tag{1}$$

Solar declination angle in month m:

$$\sin\delta_m = \sin\frac{2\pi D_m}{365}\sin(\frac{2\pi}{360}23.45) \quad m = 1,2\ldots12 \tag{2}$$

From Table 1:

Table 1. Conversion of month m, day 21, respectively, to D

m	1	2	3	4	5	6	7	8	9	10	11	12
D_m	306	337	0	31	61	92	122	153	184	214	245	275

Solar time angle:

$$\omega_t = \frac{\pi}{12}(ST_t - 12) \quad (t = 1,2\ldots5) \tag{3}$$

From Table 2, it can be seen that ST.

Table 2. Corresponding values

ST_1	ST_2	ST_3	ST_4	ST_5
9	10.5	12	13.5	15

Solar azimuth in month *m*:

$$\cos\gamma_{sm} = \frac{\sin\delta_m - \sin\alpha_{sm}\sin\varphi}{\cos\alpha_{sm}\cos\varphi} \tag{4}$$

Normal direct radiation irradiance:

$$\mathrm{DNI} = G_0[\mathrm{a} + \mathrm{b}\exp(-\frac{\mathrm{c}}{\sin\alpha_{sm}})] \tag{5}$$

$$\begin{aligned} \mathrm{a} &= 0.4237\text{-}0.00821(6\text{-}H)^2 \\ \mathrm{b} &= 0.5055\text{+}0.00595(6.5\text{-}H)^2 \\ \mathrm{c} &= 0.2711 + 0.01858(2.5 - H)^2 \end{aligned} \tag{6}$$

Where both parameters are customized in the above equation as $H = 3km$, $G_0 = 1.366kW / m^2$.

2.1.2 Solar parameter solving

The equation of the angle of declination and the equation of the solar time angle are brought into the equation of the altitude angle, which can be found out for the moment of solar altitude angle, solar azimuth and DNI for the moment of this paper are shown in **Table 2 and Table 3:**

Table 3. Solar altitude angle $\sin\alpha_s$

Solar Altitude Angle $\sin\alpha_s$					
ST	9	10.5	12	13.5	15
January	0.51	0.51	0.51	0.51	0.51
February	0.64	0.64	0.64	0.64	0.64
March	0.77	0.77	0.77	0.77	0.77
April	0.89	0.89	0.89	0.89	0.89
May	0.94	0.94	0.94	0.94	0.94
June	0.96	0.96	0.96	0.96	0.96
July	0.94	0.94	0.94	0.94	0.94
August	0.88	0.88	0.88	0.88	0.88
September	0.77	0.77	0.77	0.77	0.77
October	0.63	0.63	0.63	0.63	0.63
November	0.50	0.50	0.50	0.50	0.50
December	0.46	0.46	0.46	0.46	0.46

Table 4 Presentation of the results of the groups at special times

Time	Solar Altitude Angle α_s	Solar Azimuth Angle γ_s	**DNI (kW/m^2)**
9:00	36.33	118.93	0.97
10:30	49.42	144.09	1.03
12:00	54.90	180.00	1.04
13:30	49.42	144.09	1.03
15:00	36.33	118.93	0.97

2.2. Optical efficiency

The positional coordinates of each heliostat are visualized to obtain a scattered array, in which the total number of heliostats is 1745, with a total of 17 circles, and the positional relationship between heliostats is shown in Fig. 2.

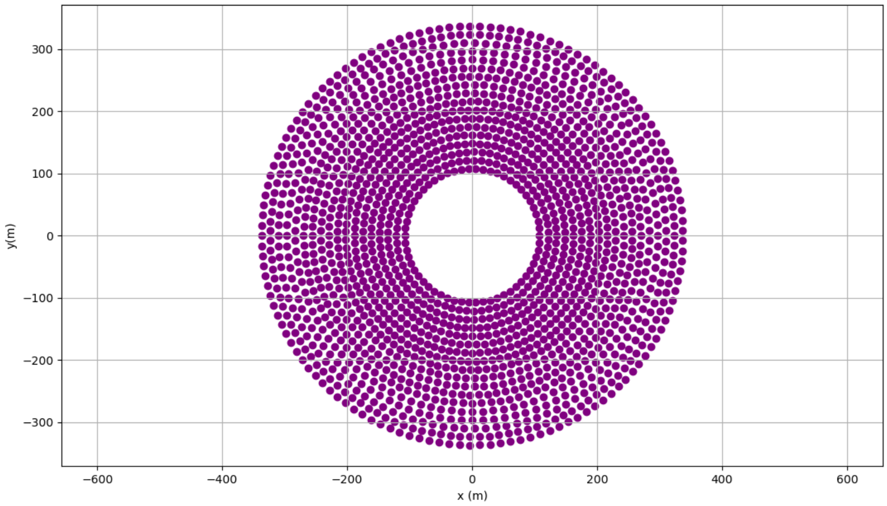

Fig. 2 Visualization of the heliostat position

Requiring the annual average optical efficiency can be done by first considering the optical efficiency of a separate heliostat, using the mirror field 3D coordinate system to find the pitch angle, and then modeling the optical losses [3]. Where the shadow obscuration loss consists of three components.

1. shadow loss caused by the tower to the mirror field.
2. Shadow loss from sunlight received by the rear sidereal mirrors being blocked by the front sidereal mirrors.
3. The light-blocking loss of the rear heliostat reflecting sunlight that is blocked by the front heliostat and does not reach the heat absorber.

2.2.1 Incident light masking model

Based on the relationship between the sun's altitude angle and the sun's azimuth angle, the incident light is represented as a vector with the following expression.

$$\overrightarrow{V_{\text{incidence}}} = (\cos\gamma_{sm}\cos\alpha_{sm}, \sin\gamma_{sm}\cos\alpha_{sm}, \sin\alpha_{sm}) \tag{7}$$

Calculation of the optical efficiency of each heliostat:

$$\eta_i = \eta_{\text{sbi}}\eta_{\text{cosi}}\eta_{\text{trunc}}\eta_{\text{ref}} \tag{8}$$

In order to calculate the optical efficiency of each heliostat, the cosine efficiency $(\eta_{\cos})$, the shadow blocking efficiency (η_{sb}), the transmittance of the atmosphere (η_{at}), and the truncation efficiency (η_{trunc}) are calculated separately for each heliostat below .

2.2.2 Atmospheric transmittance

According to the question, the following equation of equivalence exists between the atmospheric transmittance and the distance from the center of the mirror to the center of the collector.

$$\eta_{at} = 0.99231 - 0.000176 \times d_{HR} + 1.97 \times 10^{-8} \times d_{HR}^2 \quad \left(d_{HR}^2 \le 1000\right) \tag{9}$$

2.2.3 Cosine efficiency

For the analysis of the ith mirror, the light rays from the sunlight irradiated on the heliostat in the incident direction not parallel to the normal are decomposed along the normal direction and the tangent direction, respectively, where the light rays along the normal direction are the effective light rays, and the light rays along the tangent direction are the ineffective light rays, as shown in Fig. 3:

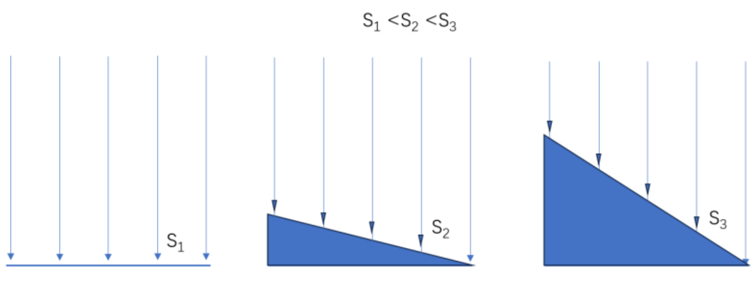

Fig. 3 Effect of pitch angle on the total light energy of the

The area S1<S2<S3, but the total amount of light energy received by them is the same.

Decomposing the light rays, the cosine efficiency is the proportion of effective light rays received, i.e., the cosine of the angle of incidence of the light rays illuminating the ith mirror, expressed as follows.

$$\eta_{\cos} = \cos(\theta_{\text{incidence}}) \tag{10}$$

2.2.4 Shadow Occlusion Efficiency

For the incident light blocking, according to the incident unit vector, the reflected light unit vector, and then find the normal vector of the mirror at this time, through the direction vector of the rod (0,0,1) and the normal vector of the cross product can be found A1B1 vector $\overrightarrow{I_{AB}}$, and then use the normal vector and $\overrightarrow{I_{AB}}$ of the cross product can be found $\overrightarrow{I_{BC}}$ vector. Finally, according to the normal vector and the height and width of the fixed-sun mirror, solve for the coordinates of the four vertices Ai, Bi, Ci and Di of the plane mirror.

At this point use the coordinates of each of the 4 vertices to find the plane equation of the plane mirror. After that, a straight line with the direction vector as the incident vector is made at the vertex of the fixed-heaven mirror. As shown in Fig. 4, IA1 is the equation of the straight line of the 1st mirror through the vertex A1, when this straight line has an intersection with the plane equations of the neighboring fixed-heaven mirrors, there is a shadow loss, and when there is no intersection, there is obviously no shadow loss.

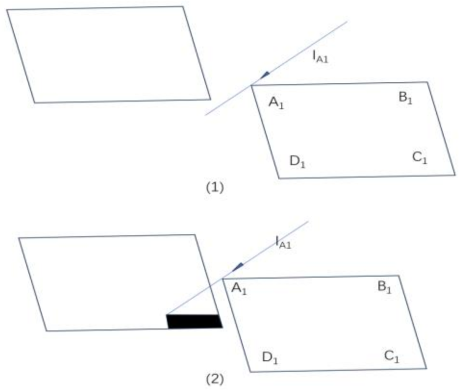

Fig. 4 Grid area analysis map

If there is a shadow loss, the Monte Carlo method is used to randomly generate a large number of grids in the plane at random, and the discrete grid of the boundary region is obtained after discretization of the boundary region is processed, and the traversal search is carried out using the Monte Carlo method [4] to find the number of discrete grids that fall within the shaded region, and to find the ratio of the area within the shaded region to the total area.

2.2.5 Calculation of luminous efficiency

The optical efficiency of each mirror was obtained by multiplying the data obtained above separately using the formula, as shown in Table 4:

Table 5. Resulting data

Date	Average Optical Efficiency	Average Cosine Efficiency	Average Shadowing Efficiency	Average Truncation Efficiency	Area-specific Average Output Thermal Power (kW/m2)
Jan 21	0.72	0.59	0.99	0.88	0.54
Feb 21	0.76	0.59	0.99	0.85	0.58
Mar 21	0.78	0.58	0.97	0.90	0.58
Apr 21	0.78	0.57	0.96	0.92	0.64
May 21	0.78	0.57	0.98	0.94	0.64
Jun 21	0.76	0.57	0.98	0.95	0.76
Jul 21	0.73	0.57	0.99	0.94	0.80
Aug 21	0.67	0.58	0.99	0.93	0.70
Sep 21	0.59	0.58	0.98	0.91	0.70
Oct 21	0.56	0.59	0.98	0.89	0.60
Nov 21	0.59	0.60	0.98	0.88	0.51
Dec 21	0.66	0.60	0.97	0.86	0.75

3. Optimization of heliostat field design

3.1. Optimization models

In the optimal design of the decision-making variables are slightly more, and the decision-making variables have a large range of changes, so the solution space is larger, if the use of traversal search cannot be searched in a limited time to the effective results, so the use of simulated annealing algorithm to achieve the solution to it [5].

Absorption tower location coordinates, heliostat dimensions, mounting height, number of heliostats, location of heliostats.

The annual power output of the mirror area of the target pole is maximized at the fixed date, i.e.

$$\max \overline{E}_{field}(\text{position coordinate、d、z、N、Position of the heliostat}) = \frac{DNI \cdot \sum_{i=1}^{N} A_i \eta_i}{\sum_{i=1}^{N} A_i} \tag{11}$$

3.1.1 Restrictive condition

a. The total output power E_{field} of the heliostat must be $60MW$.

b. The coordinates of the position of the heliostat must not exceed the assumed given circular area, which has a radius of $350m$. The position of the heliostat must not be within $100m$ of the absorption tower.

c. The distance between two adjacent heliostats should be greater than the width of the two heliostats plus $5m$.

d. The size of the fixation mirror is in $2m \sim 8m$.

e. The mounting dimensions of the fixed-sun mirror are in $2m \sim 6m$.

3.1.2 Initial parameter value setting

Location of the absorption tower: (0,0)
Number of heliostats: 1000
Fixed day mirror size: 4*m*
Fixed-sun mirror mounting height: 4*m*.
The initial coordinate range of the heliostat: $100 \le \sqrt{x_i^2 + y_i^2} \le 350$

3.1.3 Introduction of covariates and the constraints they should satisfy

Radius of the arc in which the nth circle of the heliostat is located:

$$\lambda_n = \sqrt{(x_i - x_0)^2 + (y_i - y_0)^2} \tag{12}$$

Height angle at the center of the collector relative to the nth circle of heliostats:

$$\beta = \arctan \frac{\text{Absorption tower center height - Installation height}}{\sqrt{(x_{\mathrm{i}} - x_0)^2 + (y_{\mathrm{i}} - y_0)^2}} \tag{13}$$

The distance between the mirror of the nth circle in the mirror field and its neighboring heliostat r:

$$r_n = d \times (1.749 + 0.6396\beta) + \frac{0.2873}{\beta - 0.04902} \tag{14}$$

The distance between the nth and (n+2nd) circles in the mirror field r_x:

$$r_{xn} = d \times (1.44\cot\beta - 1.094 + 3.068\beta - 1.1256\beta^2) \tag{15}$$

For the nth circle in the mirror field, the fixed-sun mirror with serial number *i*, its coordinates can be expressed as follows:

$$\begin{cases} x_i = \lambda_n \cos\alpha_i \\ y_i = \lambda_n \cos\alpha_i \end{cases} \tag{16}$$

3.2. Power optimization and position optimization

3.2.1 A brief introduction to the simulated annealing algorithm

The core idea of the simulated annealing algorithm is to take a certain temperature as a condition, change randomly between states, gradually reduce the temperature until the lowest temperature, and finally stay at the optimal solution with high probability. According to Boltzmann probability distribution can be summarized.

At the same temperature, molecules are more likely to stay in a low-energy state than a high-energy state. As the temperature increases, the difference in the probabilities of the different energy states decreases, and the probabilities of the states tend to equalize at high temperatures. As the temperature decreases, the probability of the lowest energy state gradually increases, and the probability of that state tends to 1 when the temperature tends to zero.

3.2.2 Basic solution steps of the simulated annealing algorithm

① Setting parameters, initial solutions, and decision variables.

② Perform a loop to determine if the termination condition is satisfied.

③ A set of data is then given to calculate the average annual thermal power output per unit of mirror area, and if the constraints are satisfied, then into a single.

④ Randomize the perturbation to get a new set of data, and if it is not satisfied, the process is repeated again for a loop.

⑤ Compare old and new data and update the program using Metropolis guidelines.

⑥ Determine whether to meet the unit mirror area annual average output thermal power is the largest, if the largest output results, and vice versa, return to the third step in the cycle.

3.2.3 Optimization results

The data is brought in and optimized to get the optimum design parameters, output power as well as position as shown in Table 5, Table 6, and Fig. 5:

Table 6. Annual average optical efficiency and output power table

Annual Average Optical Efficiency	Annual Average Cosine Efficiency	Annual Average Shadowing Efficiency	Annual Average Truncation Efficiency	Annual Average Output Thermal Power (MW)	Area-specific Annual Average Output Thermal Power (kW/m2)
0.69	0.60	0.98	0.94	62.18	0.63

Table 7. Table of design parameters

Absorber Tower Coordinate	Heliostat Size (Width x Height)	Heliostat Installation Height (m)	Total Number of Heliostats	Total Heliostat Area (m2)
(0, 0)	7x7	4	1050	51450

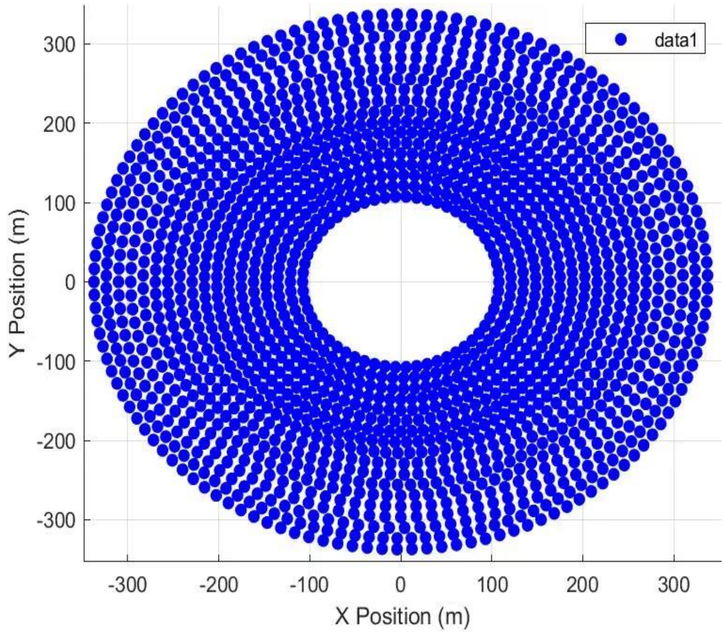

Fig. 5. Positional relationship of the heliostat obtained after optimization.

4. Summary

In this study, we developed a model for incident light obscuration of heliostats and successfully predicted their observational performance and output signals. The model has a triple advantage: first, it effectively captures the occlusion factor, which is easy to interpret and compute; second, it applies analytic geometry to transform the problem with a rigorous mathematical foundation; and third, it reduces the solution complexity by using low-level arithmetic tools. The model not only contributes to the understanding of solar activity but can also be used in areas such as computer vision and robot navigation, while providing a method for optimizing the design and production process of heliostats.

References

[1] Zhang Ligong. Research on the power scheme of heliostat in tower solar thermal power plant [J]. Solar Energy, 2019(11): 48-52.

[2] Zhang Xiaodong,Niu Haiming. Calculation model and simulation analysis of mirror field efficiency of trough-type photovoltaic power plant [J]. Distributed Energy, 2020,5(05): 56-63. DOI:10.16513/j.2096-2185.DE.2006010.

[3] Sun H, Gao B, Liu JX. Study on the layout of fixed-sun mirror field for tower solar power plant [J]. Power Generation Technology, 2021, 42(06): 690-698.

[4] Zhang, M.L. "Improved Algorithm for Shadow and Shading Efficiency of Tower Solar Heliostat Field." Proceedings of the Journal of Solar Energy, 2016, no. 8, pp. 1998-2003.

[5] LI Hongbo, FENG Guosheng, ZHU Jing et al. Thermal layout optimization of power elements based on simulated annealing algorithm [J]. Electrotechnology, 2023(13): 13-16. DOI: 10.19768/j.cnki.dgjs. 2023.13.004.